RESEARCH ARTICLE

Formulation Development and Optimisation of Quercetin Loaded Proniosomes- A Novel Herbal Drug Delivery System for Psoriasis Management

Ajay Kumar[1], Rakesh K Sindhu[2*], Satyender Kumar[1], Mohammad Rashid[3], Sumitra Singh[2]

[1]*School of Pharmacy, Sharda University, Greater Noida, Uttar Pradesh-206310, India*
[2]*Department of Pharmaceutical Sciences, Guru Jambheshwar University of Science and Technology, Hisar, Haryana-125001, India*
[3]*R.V. Northland Institute, G.B. Nagar, Dadri, Greater Noida, Uttar Pradesh-203207, India*

Received: 7th Aug, 2025; Revised: 7th Sep; Accepted: 10th Sep; Available Online: 25th Sep, 2025

ABSTRACT

Background: Psoriasis is a long-term inflammatory skin disorder marked by immunological dysregulation and keratinocyte hyperproliferation. Although quercetin, a natural flavonoid, has demonstrated strong antioxidant and anti-inflammatory properties, its clinical utility is hindered by poor water solubility and limited skin permeability. This study aimed to develop and optimize a Proniosomes delivery system to enhance the dermal delivery of quercetin for effective psoriasis management.

Methods: The thin-film hydration method was utilized for the preparation of niosomes loaded with Quercetin, using varying concentrations of cholesterol, Span 60, and soya lecithin. Box–Behnken design was employed to optimize key formulation parameters, targeting minimized particle size, enhanced zeta potential, and maximized drug release. The optimized formulation was characterized for entrapment efficiency (EE%), particle size, *in-vitro* drug release, *ex-vivo* skin permeation, and FTIR compatibility studies.

Results: FTIR analysis confirmed the absence of significant drug–excipient interactions. The optimal region was identified which demonstrated high drug release (87%), favorable particle size (275 nm), and excellent zeta potential (-39 mV). The percent entrapment efficiency (% EE) of the optimized formulation was found to be 70.79±5.63%, indicating the preparation method of Proniosomes is good and has the potential for scalability. The study highlights the importance of surfactant concentration in controlling drug release and the need for further optimization in the formulation. *In-vitro* studies demonstrated an efficient and excellent sustained release formulation profile, reaching nearly ~100% over 24 hours, compared to <20% from pure quercetin.

Conclusion: Quercetin-loaded Proniosomes effectively enhanced the solubility, stability, and skin penetration of the drug, supporting their potential as a scalable and effective transdermal delivery system for herbal therapy in psoriasis. Further *in-vivo* studies over the developed nano carrier as Proniosomes are warranted to establish therapeutic efficacy and safety in clinical settings.

Keywords: Quercetin, Proniosomes, Psoriasis, Optimization, Box-Behnken Design (BBD)

How to cite this article: Ajay Kumar, Rakesh K Sindhu, Satyender Kumar, Mohammad Rashid, Sumitra Singh. Formulation Development and Optimisation of Quercetin Loaded Proniosomes- A Novel Herbal Drug Delivery System for Psoriasis Management. International Journal of Drug Delivery Technology. 2025;15(3):1065-76. doi: 10.25258/ijddt.15.3.22

Source of support: Nil.

Conflict of interest: None

INTRODUCTION

Psoriasis is a long-term, immune-mediated inflammatory skin condition that causes erythematous, scaly plaques that severely lower quality of life[1]. Psoriasis is a common disease with a geographical-prevalence range of 0.50% to 11 % in adults and 0.00 % to 1.35% in children, but limited data on its epidemiology and geographic distribution[2,3]. It is typified by keratinocyte hyperproliferation and abnormal differentiation[4]. Conventional treatment methods, such as systemic immunosuppressants, phototherapy, and topical corticosteroids, are frequently constrained by side effects, resistance, and low patient compliance, particularly when used for an extended period of time[5-8]. Plant-derived bioactive compounds with good safety profiles and a variety of therapeutic effects are therefore gaining popularity[9].

As a systemic inflammatory illness, psoriasis often coexists with a number of other disorders, including metabolic syndrome, diabetes, essential hypertension, and inflammatory bowel disease[10,11]. Abnormal immunomodulatory processes and common inflammatory pathways may be the cause of these disorders' associations[12]. A naturally occurring flavonoid that is found in large quantities in fruits and vegetables, quercetin has shown strong anti-inflammatory, antioxidant, and immunomodulatory type of response, making viable option

**Author for Correspondence: drrakeshksindhu@gmail.com*

for the treatment of psoriasis [13-15]. However, its limited skin permeability, low stability, and poor water solubility make it difficult to use therapeutically in topical formulations. Delivery systems based on nanotechnology[16,17], like Proniosomes, have become a new and promising way to get around these restrictions[18,19]. Proniosomes are free-flowing, dry formulations that, when hydrated, can transform into niosomes, providing improved skin penetration, prolonged drug release, and increased drug stability[20,21]. Proniosomes can help localize drug delivery to psoriatic lesions while reducing systemic exposure when they are loaded with phytoconstituents like quercetin[22,23].

The formulation, development, and optimization of quercetin-loaded Proniosomes as a novel herbal drug delivery system for the treatment of psoriasis are the main objectives of this study[24-26]. The study intends to maximize entrapment efficiency, optimal vesicle size, and desired drug release characteristics by optimizing key formulation parameters using a quality-by-design (QbD) approach. However, in order to attain desired physicochemical properties the formation of stable and effective Proniosomes necessitates careful optimization of crucial formulation and process parameters (CMPs)[27]. The amount of Span (X_1), soy lecithin (X_2), and cholesterol (X_3) were found to be the three main variables that significantly influenced the stability and functionality of Proniosomes in this investigation[28]. The study utilized a nonlinear second-order Box-Behnken Design (BBD) to analyze and optimize parameters, allowing for systematic investigation of interactions between factors. A total of 17 experimental trials were conducted, each representing a different combination of chosen parameters. The best conditions for nanoparticle formation were identified by evaluating the formulations for their primary quality criteria.

The results of this study could lead to the creation of more patient-friendly, potent herbal treatments for inflammatory skin conditions like psoriasis[29]. It can be concluded as it is a serious dermatological disorder that harms both the body and the mind is psoriasis[30]. Skin atrophy and systemic toxicity are side effects of current treatments like immunomodulators and corticosteroids[31]. Long-term use of alternative herbal therapies is becoming more and more popular. Preclinical research has indicated promise for quercetin, a flavonoid with anti-inflammatory, antioxidant[27], and immunosuppressive qualities[32]. However, physicochemical limitations limit its clinical utility. A stable precursor to niosomes, Proniosomes can enhance drug entrapment, permeation, and sustained release, thereby enhancing patient adherence and therapeutic efficacy[33]. A safer and more efficient way to treat psoriasis may be to incorporate quercetin into a proniosomal delivery system.

MATERIALS AND METHODS

Materials

Quercetin (≥98% purity) was obtained from a reputable supplier of phytochemicals. Span 60 (sorbitan monostearate) and cholesterol were sourced from Sigma-Aldrich (USA). Ethanol of analytical grade and additional solvents were acquired from Merck, India. All chemicals and reagents utilized in this study were of analytical grade and employed without additional purification. Deionized water was utilized consistently during the experiments. A dialysis membrane with a molecular weight cut-off of 12,000–14,000 Da was acquired from HiMedia Laboratories, Mumbai.

Table 1: BBD design[36]. Coded and actual levels of independent formulation variables used in the design of experiments. Each factor was studied at three levels: low (–1), medium (0), and high (+1)

Variable	-1	0	+1
Cholesterol	0.10	0.15	0.20
Span 60	0.150	0.375	0.600
Soya lecithin	0.1	0.2	0.3

Analysis Method

By creating a number of standard solutions with concentrations ranging from 1 to 10 µg/mL in methanol, a standard calibration curve of quercetin was created. A UV-Visible spectrophotometer was used to measure each solution's absorbance at λmax=370 nm in comparison to a reagent blank[34]. The standard curve (Figure 1) demonstrated a strong linear relationship between the resulting absorbance values and concentration. With a correlation coefficient (R^2) and linear regression equation was developed. The quercetin content of formulation samples, including entrapment efficiency and *in-vitro* drug release studies, was then ascertained using this equation[29,35].

Fourier-Transform Infrared (FTIR) Spectroscopy

The FTIR analysis was performed on a Bruker FT-IR VERTEX 80/80 v (Boston, MA, USA) in Attenuated Total Reflectance mode (ATR) with a platinum crystal accessory between 400 and 4000 cm^{-1}, a resolution of 4 cm^{-1} and 16 scans.

Experimental Design and Optimization

A Box Banken design (BBD) approach using a quadratic relationship was employed to investigate the effect of key formulation variables. Statistical analysis and optimization were performed using Design-Expert® software (Stat-Ease Inc., USA).

Three key formulation variables-Cholesterol, Span 60, And Soya Lecithin were selected for optimization using a three-level design. Each variable was studied at low (–1), medium (0), and high (+1) concentration levels to evaluate their effects on particle size, zeta potential, and drug release from the proniosomal system, Table 1.

Method of Preparation for Quercetin Proniosomes

The thin-film hydration method was utilized for the preparation of niosomes. Quercetin (50 mg) was dissolved in 20 mL of chloroform, followed by the addition of adequate amount of Span 60, cholesterol, and soya lecithin. The mixture was thoroughly dissolved and transferred into a round-bottom flask (RBF). The RBF was then placed on a rotary evaporator at 60°C, where the solvent gradually evaporated, forming a thin lipid film on the inner surface of the flask. The flask was kept undisturbed for 24 hours to ensure complete removal of residual solvent. After one day, the dried film was hydrated by adding an appropriate

volume of distilled water with continuous shaking, leading to the formation of niosomal vesicles[37,38].

Particle Size and Zeta Potential Determination

The hydrodynamic diameter (average size), polydispersity index (PDI) and zeta potential of the optimized Proniosomes were determined by dynamic light scattering (Zetasizer Nano ZS, Malvern Instruments, Malvern, UK). The samples were analyzed in a folded capillary cell. Detection of the scattered light was carried out at 173° (NIBS = non-invasive backscatter detection) and temperature of 25 °C. The zeta potential was measured by laser Doppler micro-electrophoresis using the same Zetasizer ZS Nano. The samples were filtered with 0.45 µm syringe filter (Minisart® High Flow, Sartorius, Gloucestershire, UK) to eliminate eventual particles above 450 nm and compared to the samples without filtering. At least five replicates were performed for each sample and the results were given as mean ± standard deviation of the obtained values.

Vesicle Size and Zeta Potential

The average particle size, polydispersity index (PDI), and zeta potential of hydrated proniosomal vesicles were measured using dynamic light scattering (DLS) with a Zetasizer Nano ZS (Malvern Instruments, UK).

In-vitro Drug Release

Drug release was studied using the dialysis membrane diffusion technique. The hydrated proniosomal suspension was placed in a pre-soaked dialysis bag and suspended in PBS (pH 7.4) at 37 ± 0.5 °C under constant stirring. Samples were withdrawn at predefined intervals, filtered, and analyzed spectrophotometrically.

The optimal preparation of quercetin loaded Proniosomes were studied using the dialysis bag (M.W.: 12,000 Da) method, with a 50% ethanol and 50% phosphate buffer (50:50; PBS, pH 6.8) mixture as the dissolution medium. The dialysis bag was first filled with 10 mL of proniosomal formulation after being immersed in PBS (pH 6.8) for a full day. After that, the dissolving medium was added, mixed, and kept at 37 ± 0.5 °C while being magnetically agitated at 100 rpm. After that, 2 mL of the dissolution medium was

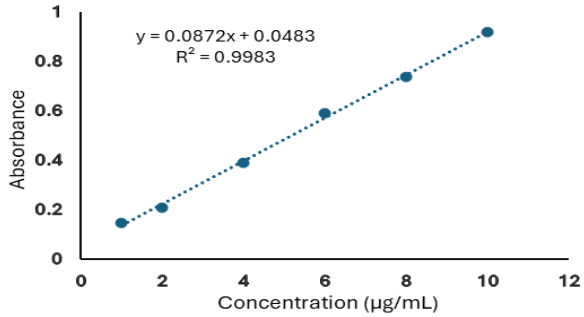

Figure 1: Standard calibration curve of quercetin in methanol at 370 nm

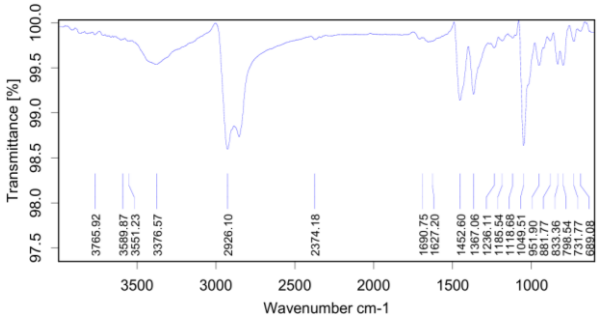

Figure 2: FTIR of Cholesterol

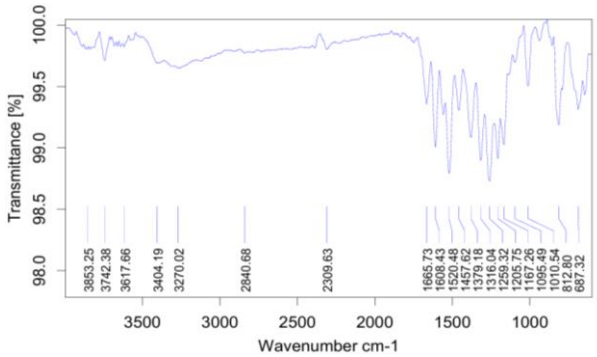

Figure 3: FTIR of Quercetin

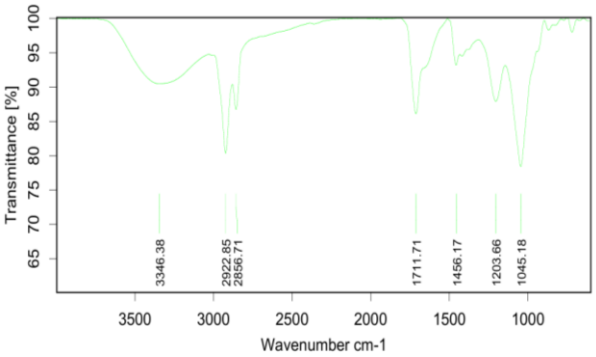

Figure 4: FTIR of Lecithin

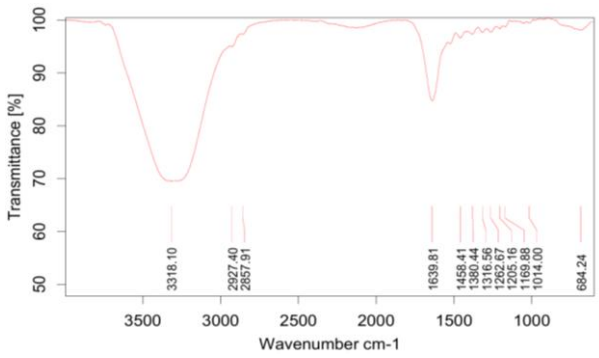

Figure 5: FTIR of Quercetin

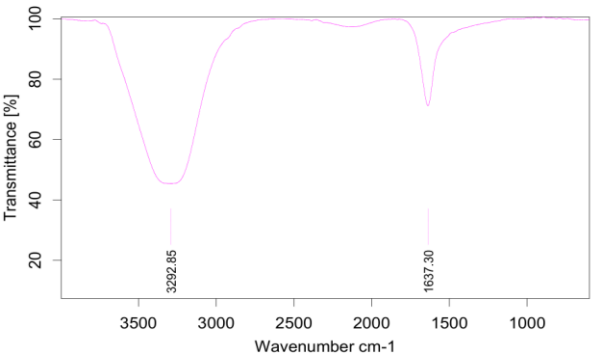

Figure 6: FTIR of Physical Mixture Quercetin loaded Proniosomes

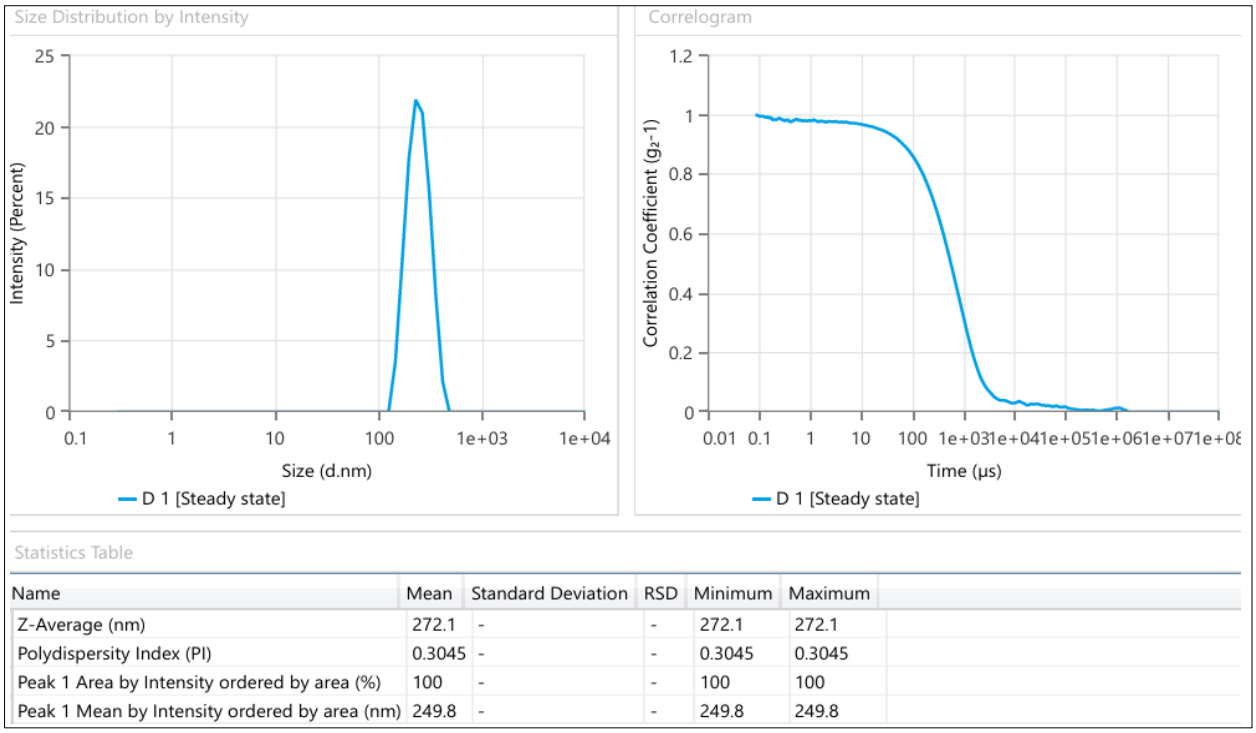

Statistics Table

Name	Mean	Standard Deviation	RSD	Minimum	Maximum
Z-Average (nm)	272.1	-	-	272.1	272.1
Polydispersity Index (PI)	0.3045	-	-	0.3045	0.3045
Peak 1 Area by Intensity ordered by area (%)	100	-	-	100	100
Peak 1 Mean by Intensity ordered by area (nm)	249.8	-	-	249.8	249.8

Figure 7: Z-Average of Proniosomes vesicles

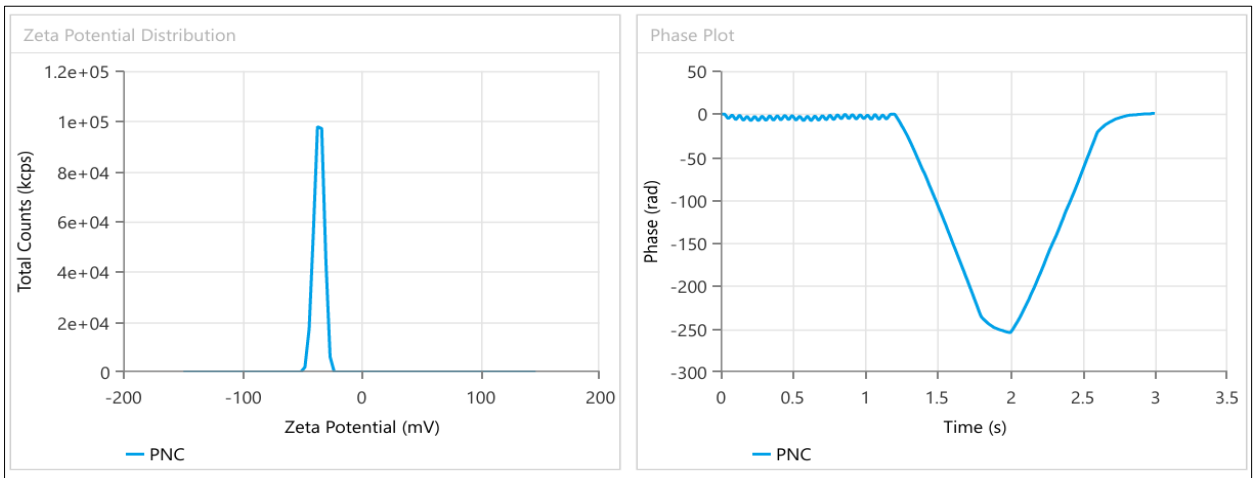

Statistics Table

Name	Mean	Standard Deviation	RSD	Minimum	Maximum
Zeta Potential (mV)	-35.59	-	-	-35.59	-35.59
Zeta Peak 1 Area (%)	100	-	-	100	100
Zeta Peak 1 Mean (mV)	-35.59	-	-	-35.59	-35.59
Derived Mean Count Rate (kcps)	3.697E+05	-	-	3.697E+05	3.697E+05
Mean Count Rate (kcps)	606.2	-	-	606.2	606.2
Conductivity (mS/cm)	0.6908	-	-	0.6908	0.6908

Figure 8: Zeta-Potential of Proniosomes

withdrawn and replaced at different intervals of time with the same amount of fresh dissolution medium.

UV spectrophotometric analysis was performed at 382 nm to measure the concentration of quercetin release form the proniosomal formulation. The study was performed in triplicate and the results were shown as (mean ± standard deviation)[34].

Entrapment Efficiency (%EE)

Entrapment efficiency was determined by centrifuging the hydrated Proniosomes at 14,000 rpm for 60 min at 4 °C. The free, unentrapped quercetin in the supernatant was quantified using UV-visible spectrophotometry at 370 nm. The amount of integrated quercetin (% EE) at 382 nm was measured using an UV-Vis Spectrophotometer (2202, Systronics, Mumbai, India) after the aqueous dispersion had been run through a 0.45 m syringe filter. The quantity of quercetin was calculated by subtracting the amount of

Table 2: *In-vitro* Drug Release of RUN 14

S. No.	Time (h)	Mean area (n=3)*	Concen. (µg/ml)	Cumulative amount of drug permeation (µg)	Cumulative percentage of drug permeation (%)	Cumulative amount of drug permeation (µg/cm^2)	J-Flux (µg/cm^2/h)	P_b x 10^2	R2
1	1	116796	1.8	180	3.6	60.00	60.42	1.208333	0.9855
2	2	363365	5.6	560	11.2	186.67			
3	3	655355	10.1	1010	20.2	336.67			
4	4	1096585	16.9	1690	33.8	563.33			
5	5	1401552	21.6	2160	43.2	720.00			
6	6	1738963	26.8	2680	53.6	893.33			
7	7	2095839	32.3	3230	64.6	1076.67			
8	8	2296988	35.4	3540	70.8	1180.00			
9	10	2537069	39.1	3910	78.2	1303.33			
10	12	2673331	41.2	4120	82.4	1373.33			
11	24	2822570	43.5	4350	87	1450.00			

Table 3: BBD design, Runs of the Formulations[36], Experimental design matrix showing the levels of cholesterol, Span 60, and soya lecithin used in each run, along with the corresponding measured responses: particle size, zeta potential, and drug release from the formulated proniosomal system

Run	Chole-sterol	Span 60	Lecithin	Particle Size (nm)	Zeta Potential (mV)	Drug Release (%)
1	0.20	0.375	0.30	275	-39	87
2	0.15	0.375	0.20	290	-37	86
3	0.20	0.375	0.10	356	-34	78
4	0.15	0.375	0.20	268	-38	84
5	0.20	0.150	0.20	375	-31	80
6	0.15	0.600	0.10	455	-25	67
7	0.10	0.375	0.10	293	-35	82
8	0.15	0.150	0.10	215	-22	69
9	0.10	0.150	0.20	224	-21	65
10	0.15	0.600	0.30	476	-23	72
11	0.15	0.150	0.30	210	-21	64
12	0.20	0.600	0.20	465	-26	74
13	0.10	0.375	0.30	245	-31	86
14	0.15	0.375	0.20	268	-32	87
15	0.10	0.600	0.20	433	-23	73
16	0.15	0.375	0.20	257	-35	84
17	0.15	0.375	0.20	274	-34	85

original drug from the amount of free drug, after the determination of the amount of unentrapped quercetin in the filtrate[39].

RESULTS AND DISCUSSION

Standard Calibration Plot of Quercetin

The calibration curve for quantifying quercetin in solution is represented by a linear regression equation with a slope of 0.0872 and a y-intercept of 0.0483.

$y = 0.0872x + 0.0483$

The coefficient of determination is $R^2 = 0.9983$, indicating the data's fit to the linear model. A number around 1 signifies a superior linear correlation between absorbance and concentration, rendering the method exceptionally dependable and precise for quantifying quercetin in solution (Figure 1). The calibration curve enables the determination of unknown quercetin concentrations in diverse samples, including drug release and entrapment efficiency investigations, by substituting absorbance values into the equation and resolving for x.

Table 4: BBD design, Response summary of the Formulations[36]

Response	Mean	Min	Max	Std. Dev.
Particle Size (nm)	316.1	210	476	± 83.3
Zeta Potential (mV)	-30.2	-21	-39	± 6.2
Drug Release (%)	77.1	64	87	± 7.6

Fourier-Transform Infrared (FTIR) Spectroscopy

FTIR Spectroscopy was employed to identify the primary functional groups in the formulation's individual components and to verify their structural integrity.

The FTIR spectrum of cholesterol (Figure 2) displayed characteristic peaks at 3400 cm^{-1}, indicative of O–H stretching vibrations, alongside strong bands between 2800 and 3000 cm^{-1}, which are associated with symmetric and asymmetric C–H stretching of CH_2 and CH_3 groups. A prominent peak at 2899 cm^{-1} signified CH_2 symmetric stretching, whereas a clear signal at 1690 cm^{-1} validated the existence of C=C stretching from the unsaturated bond in the second ring of the cholesterol structure.

The spectrum of Span 60 (Figure 3) exhibited significant absorption bands at 3452 cm^{-1} (O–H stretching), 2800–3000 cm^{-1} (C–H stretching), and 1250 cm^{-1} (C–O stretching), which suggests the presence of hydroxyl and ester functionalities. Soya lecithin (Figure 4) exhibited significant peaks at 2854 cm^{-1} and 2928 cm^{-1}, corresponding to symmetric and asymmetric CH_2 stretching, respectively. Additionally, bands were observed at 2956 cm^{-1} for CH_3 stretching and at 1462 cm^{-1} for CH_2 scissoring. The carbonyl (C=O) stretch was recorded at 1736 cm^{-1}, while phosphate-related vibrations (PO_2^- and P–O–C) were detected in the range of 1200 to 970 cm^{-1}, with a notable peak around 1045 cm^{-1}, thereby confirming the phospholipid structure.

Quercetin, (Figure 5) a representative flavonoid, displayed O–H stretching vibrations at 3406 cm^{-1} and 3283 cm^{-1}, along with a phenolic O–H bending at 1379 cm^{-1}. The aryl ketonic C=O stretch was observed at 1666 cm^{-1}, and aromatic C=C stretching vibrations were detected at 1610, 1560, and 1510 cm^{-1}.

The presence of additional bands at 1317 cm^{-1} (C–H in-plane bending) and at 933, 820, 679, and 600 cm^{-1} (out-of-plane bending) further substantiates its polyphenolic

Table 5: BBD design, Regression coefficients and corresponding p-values for the influence of independent variables and their interactions on particle size, zeta potential, and drug release in the developed proniosomal formulation. Statistically significant terms ($p < 0.05$) are highlighted, indicating key factors affecting each response variable[36]

	Intercept	A	B	C	AB	AC	BC
Particle size	271.4	23.25	126.5	4	-29.75	-8.25	6.5
p-values		0.0183	< 0.0001	0.5439	0.0079	0.2436	0.3423
Zeta Potential	35.2	2.5	0.25	-0.25	-1.75	2.25	-0.25
p-values		0.0182	0.7683	0.7683	0.1732	0.0922	0.8347
Release	85.2	-0.75	1.5	1.44252E-15	-3.5	1.25	2.5
p-values		0.3141	0.0829	1.0000	0.0058	0.1277	0.0185
	Intercept	A^2	B^2	C^2	A^2B	A^2C	AB^2
Particle size	271.4	28.05	74.8	-7.2	-51.75	-36.25	22.5
p-values		0.0089	0.0002	0.2883	0.0037	0.0132	0.0579
Zeta Potential	35.2	1.025	-10.975	-1.475			
p-values		0.3925	< 0.0001	0.2312			
Release		1.525	-13.725	-3.475	-1	3.25	4.75
p-values		0.0744	< 0.0001	0.0054	0.3391	0.0243	0.0067

Table 6: BBD design, Constraints[36]

Name	Goal	Lower Limit	Upper Limit	Lower Weight	Upper Weight	Importance
A: Cholesterol	is in range	0.1	0.2	1	1	3
B: Span 60	is in range	0.15	0.6	1	1	3
C: Soya lecithin	minimize	0.1	0.3	1	1	2
Particle size	minimize	210	476	1	0.1	1
Zeta Potential	maximize	21	39	0.524807	1	2
Release	maximize	64	87	0.549541	1	4

Table 7: BBD design, Constraints Solutions found[36]

Number	Cholesterol	Span 60	Soya lecithin	Particle size	Zeta Potential	Release	Desirability	
1	0.109	0.384	0.103	281.460	34.526	82.436	0.911	Selected
2	0.109	0.384	0.103	282.053	34.538	82.441	0.911	
3	0.110	0.384	0.103	280.889	34.516	82.453	0.911	
4	0.123	0.379	0.100	264.159	34.160	82.307	0.910	

structure. The peaks observed at 1263, 1200, and 1165 cm^{-1} correspond to C–O stretching in aryl ethers, phenols, and ketonic moieties, respectively.

Interpretation for FTIR of Final Formulation

The FTIR spectrum of the optimized quercetin-loaded proniosomal formulation (Figure 6) was recorded to assess potential drug-excipient interactions and confirm the incorporation of quercetin into the lipid-based system.

The spectrum revealed a broad and strong absorption peak at 3292.85 cm^{-1}, which corresponds to O–H stretching vibrations. This peak is characteristic of both quercetin's hydroxyl groups and Span 60/cholesterol's hydrophilic moieties, suggesting possible hydrogen bonding between the drug and lipid carriers. Another distinct peak was observed at 1637.30 cm^{-1}, which may be attributed to the C=O stretching vibration or C=C aromatic ring stretch, indicating the presence of quercetin's aryl ketone structure. The absence of any new or shifted peaks compared to the individual spectra of the drug and excipients suggests that no major chemical interaction occurred. However, the preservation of quercetin's characteristic peaks, albeit with slight broadening, supports successful entrapment of the drug within the Proniosomes matrix in a stable form.

The absence of prominent peaks corresponding to quercetin in the FTIR spectrum of the formulation suggests successful encapsulation within the Proniosomes system. This indicates that quercetin is incorporated into the lipid or surfactant matrix, reducing its free presence and characteristic spectral signals.

Vesicle Size and Zeta Potential

Average particle size of the optimized formulation of quercetin loaded Proniosomes was found to be 272.1 nm (Figure 7) with a PDI of 0.304 suggesting a uniform, monodisperse population, meaning the prepared

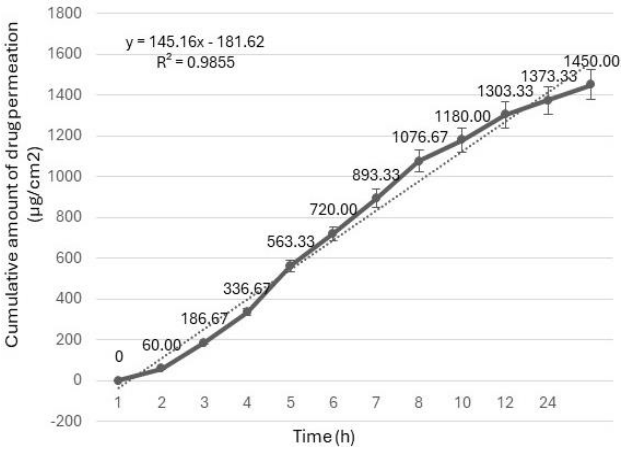

Figure 9: Graph for Drug release from Proniosomes RUN 14

Proniosomes are relatively similar in size, with low variation. Span 60 (Sorbitan monostearate) generally imparts a negative zeta potential (Figure 8) to vesicles like Proniosomes or niosomes. This occurs because of presence of Span 60, a non-ionic surfactant, has a slight negative charge due to its stearic acid moiety. It can also adsorb hydroxyl ions from water, resulting in a net negative charge on the vesicle surface. Span 60's lack of a strong cationic group creates a slightly negative zeta potential, which increases stability due to electrostatic repulsion between vesicles and reduces aggregation and flocculation in dispersion systems.

In-vitro Drug Release Study of Formulations[40]

The *in-vitro* skin permeation study revealed a consistent increase in drug permeation over 24 hours. The cumulative amount of drug permeated through the membrane exhibited a linear relationship with time, as shown in Figure 9[41]. The linear regression equation was:

$$y = 123.37x$$

$$R^2 = 0.9869$$

where y represents the cumulative amount of drug permeated (µg/cm²) and x denotes time (h). The high R^2 value indicates a strong linear correlation, suggesting a controlled and sustained release profile[42].

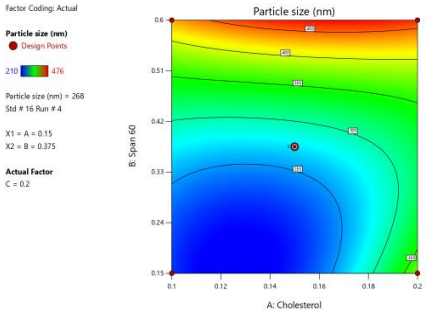

Figure 10: Contour plot representing the effect of cholesterol (A) and Span 60 (B) on particle size (nm) of quercetin-loaded Proniosomes

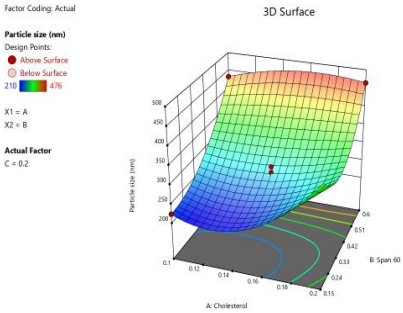

Figure 11: Three-dimensional surface plot illustrating the combined influence of cholesterol (A) and Span 60 (B) on the particle size (nm) of quercetin-loaded Proniosomes

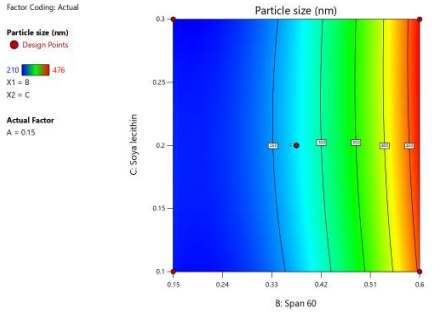

Figure 12: Contour plot representing the effect of Soya lecithin (A) and Span 60 (B) on particle size (nm) of quercetin-loaded Proniosomes

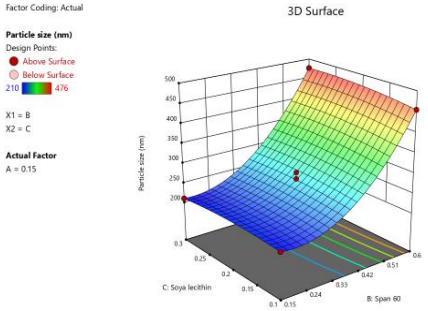

Figure 13: Three-dimensional surface plot illustrating the combined influence of Soya lecithin (A) and Span 60 (B) on the particle size (nm) of quercetin-loaded Proniosomes

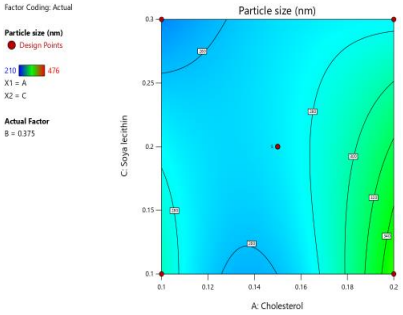

Figure 14: Contour plot representing the effect of cholesterol (A) and Soya lecithin (B) on particle size (nm) of quercetin-loaded Proniosomes

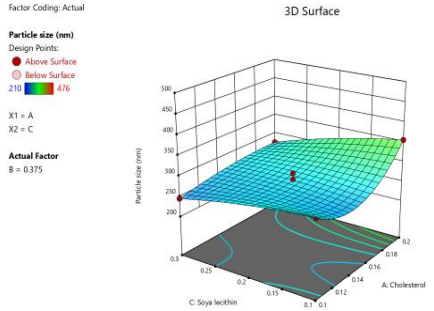

Figure 15: Three-dimensional surface plot illustrating the combined influence of cholesterol (A) and Soya lecithin (B) on the particle size (nm) of quercetin-loaded Proniosomes

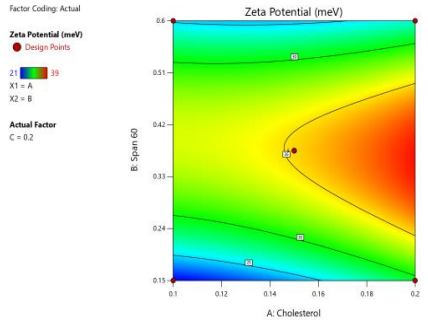

Figure 16A: Contour plot representing the effect of cholesterol (A) and Span 60 (B) on Zeta-Potential (mV) of quercetin-loaded Proniosomes

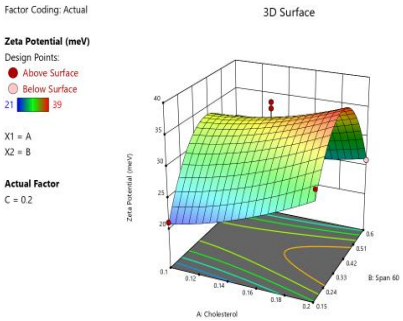

Figure 16B: Three-dimensional surface plot illustrating the combined influence of cholesterol (A) and Span 60 (B) on the Zeta-Potential (mV) of quercetin-loaded Proniosomes

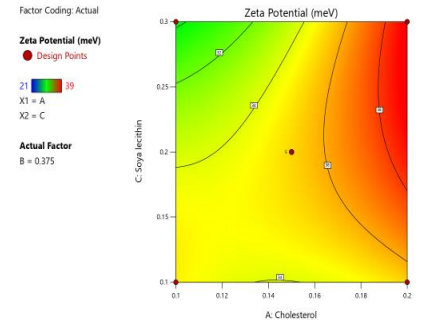

Figure 17: Contour plot representing the effect of cholesterol (A) and Soya lecithin (B) on Zeta-Potential (mV) of quercetin-loaded Proniosomes

The calculated steady-state flux (J) was 145.16 µg/cm²/h, which reflects the efficiency of the Proniosomes formulation in enhancing transdermal delivery of quercetin (Table 2, Figure 9).

A total of 17 experimental runs (Table 3) were carried out based on a response surface methodology design to evaluate the influence of formulation variables—cholesterol, Span 60, and soya lecithin—on key physicochemical parameters. The responses measured included particle size (nm), zeta potential (mV), and cumulative drug release (%), which were used to develop and validate the statistical model for optimization.

Experimental Design and Optimization[43]

A three-factors and three-levels containing BBD was employed for the optimization.

With increase in span and cholesterol concentration particle size increased which can be attributable to that interfacial tensions may have increased leading to bigger droplet size. With increasing soya lecithin, the particle size hardly showed any change as span 60 conc was sufficient enough to produce small size formulation. While moving from low

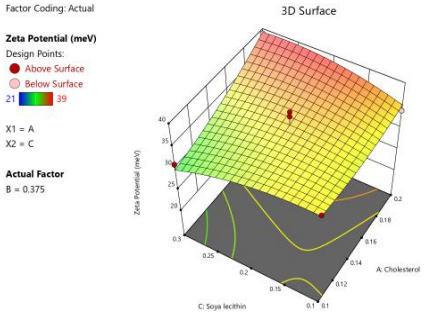

Figure 18: Three-dimensional surface plot illustrating the combined influence of cholesterol (A) and Soya lecithin (B) on the Zeta-Potential (mV) of quercetin-loaded Proniosomes

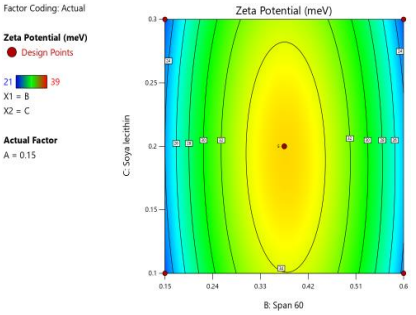

Figure 19: Contour plot representing the effect of Soya lecithin (A) and Span 60 (B) on Zeta-Potential (mV) of quercetin-loaded Proniosomes

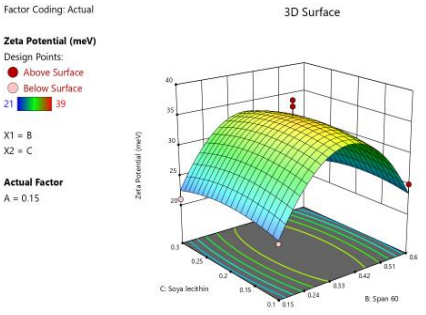

Figure 20: Three-dimensional surface plot illustrating the combined influence of Soya lecithin (A) and Span 60 (B) on the Zeta-Potential (mV) of quercetin-loaded Proniosomes

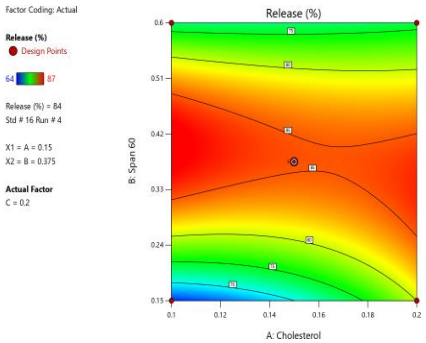

Figure 21: Contour plot representing the effect of cholesterol (A) and Span 60 (B) on Release (%) of quercetin-loaded Proniosomes

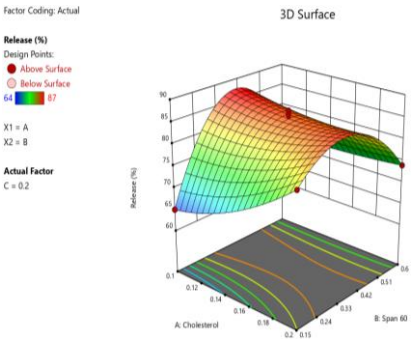

Figure 22: Three-dimensional surface plot illustrating the combined influence of cholesterol (A) and Span 60 (B) on the Release (%) of quercetin-loaded Proniosomes

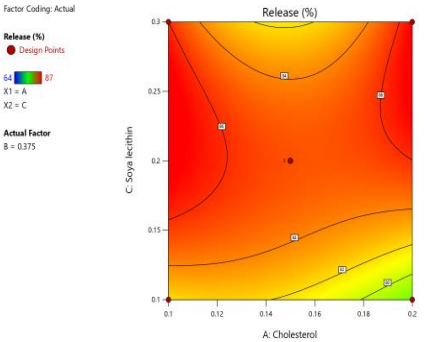

Figure 23: Contour plot representing the effect of cholesterol (A) and Soya lecithin (B) on Release (%) of quercetin-loaded Proniosomes

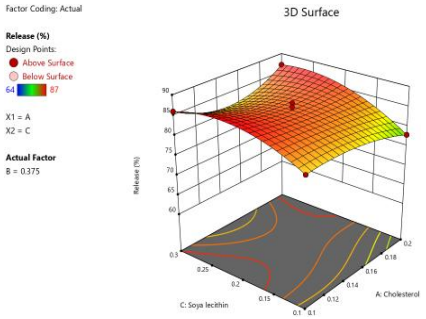

Figure 24: Three-dimensional surface plot illustrating the combined influence of cholesterol (A) and Soya lecithin (B) on the Release (%) of quercetin-loaded Proniosomes

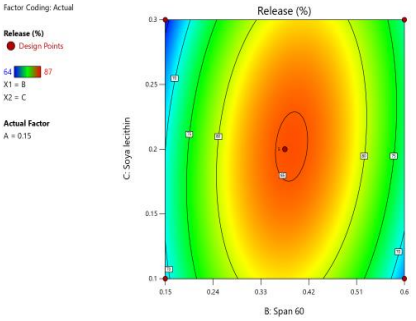

Figure 25: Contour plot representing the effect of Soya lecithin (A) and Span 60 (B) on Release (%) of quercetin-loaded Proniosomes

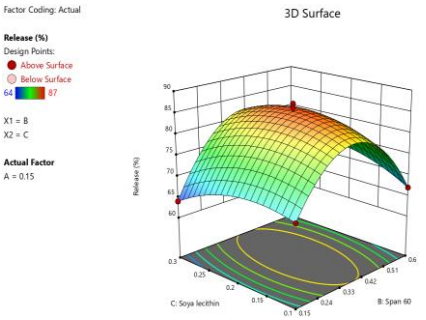

Figure 26: Three-dimensional surface plot illustrating the combined influence of Soya lecithin (A) and Span 60 (B) on the Release (%) of quercetin-loaded Proniosomes

to high levels of span 60, the particle size increased which is similar to observation with cholesterol concentration.
Likewise, Soya lecithin does not show remarkable change sin particle size, while cholesterol showed little increase in particle size with its increasing concentration.
Niosomes with low zeta potential values are more susceptible to aggregation and potential destabilization. With increase in span concentration initially zeta potential increased, however at the highest levels it exhibited lower values of zeta indicating an unstable formulation. This could be attributed to the fact that the mid values of span were sufficient enough to produce a stable formulation. The values of zeta potential were found to be maximum for intermediate values of soya lecithin, while there was little effect of cholesterol concentration (figure 17)
There was miniscule effect of cholesterol and soya lecithin concentration on zeta potential. This may be attributed to span 60 concentrations, being the surfactant was solely responsible for stability of the formulation.
The graph typically showed dome like structure. This means the mid values of span 60 were sufficient to produce monodisperse formulation with high zeta potential (figure16A and B)
The % drug release values were found to low at low and high values of span and low levels of cholesterol. This could be attributable to the fact that higher concentrations of cholesterol and mid values of span were able to produce monodispersion of particles with minimum heterogeneity and high drug solublisation resulting in higher drug release.
Soya lecithin and cholesterol concentration showed little effect on quercetin release. Though their concentration effect the drug solubility, yet concentration of surfactant at the same time is responsible for controlling the release.
Akin observation of effect of span and soya lecithin were observed on drug release as that of zeta potential (Figure 26). The concentration of span 60 at mid values produced higher drug release owing to optimum solubility of quercetin in the blend of surfactant, lipid and cholesterol.
The constraints were further narrowed down to demarcate the design space in the overlay contour plot between the chosen three factors across 2D experimental domains. The latter depicts the desirable optimal design space region in the yellow colour, surrounded with the grey colour region, called the knowledge space.

Coefficients Table

Multiple linear regression technique was employed, followed by fitting of the data with an apt polynomial model. Interaction terms and aptness of model fitting were studied using statistical parameters. Response surface mapping was carried out by employing 2D and 3D graphs to understand the relationship(s) among the CMAs and studied CQAs. The projection of optimum formulation was carried out by using desirability and design space as the functions of numerical and graphical optimisation, respectively.
Factors A and B and their interactions are critical for controlling particle size. Quadratic and higher-order effects also play substantial roles, indicating that optimization is needed rather than linear extrapolation. Zeta potential is primarily affected by the linear effect of A and the quadratic term C^2. Stability is likely influenced by these two. Drug release is influenced by complex interactions and quadratic effects. Especially notable is the strong impact of the C^2 term, suggesting this factor requires tight control in formulation.
Factor A (e.g., surfactant) plays a critical role across particle size, zeta potential, and drug release. Quadratic terms (especially C^2 and B^2) and interactions (AB, BC) are prominent, indicating non-linear relationships. This validates the use of Response Surface Methodology (RSM) and suggests that simple linear models would not adequately capture the formulation behaviour (Table 4).

Numerical Desirability and Numerical Optimization

The optimum formulation was earmarked employing numerical desirability function, by “trading off” various CQAs for achieving the required goals, i.e. minimum particle size (i.e., representing the rapidness absorption) and maximum zeta potential (i.e., demonstrating adequate stability), and maximum percent release (i.e., necessary for quercetin release) (Table 5,6).
Overlay plots (Figure 27) were generated using response surface methodology (RSM) to identify the optimal design

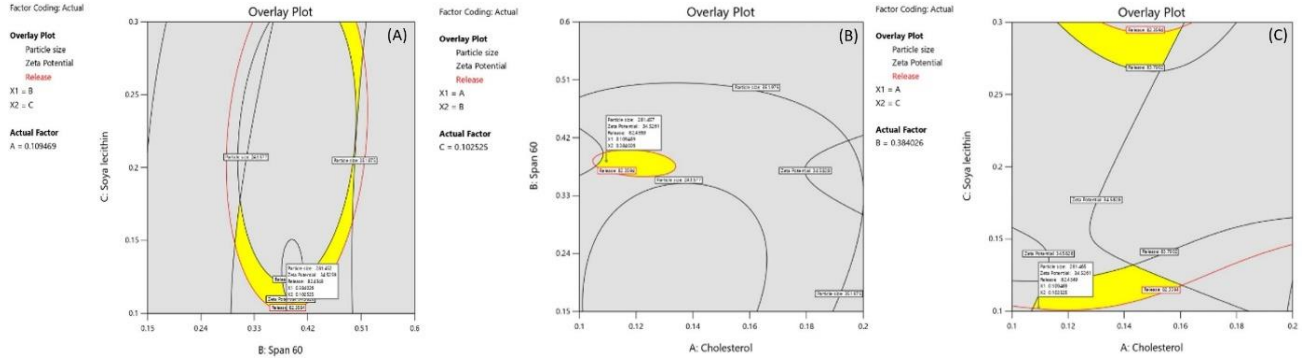

Figure 27: Overlay plots representing the optimization of quercetin-loaded proniosomal formulations using response surface methodology (RSM). The yellow regions in each plot denote the design space where all three critical quality attributes-minimized particle size, optimal zeta potential, and maximum drug release-are simultaneously satisfied. (A) Overlay plot of Span 60 vs. soya lecithin with cholesterol held constant at 0.1095 g; (B) Overlay plot of cholesterol vs. Span 60 with lecithin held at 0.1025 g; (C) Overlay plot of cholesterol vs. soya lecithin with Span 60 fixed at 0.3480 g. These plots collectively identify the optimal formulation region suitable for enhanced topical delivery of quercetin in psoriasis therapy

space for the quercetin-loaded proniosomal formulation. The plots concurrently assessed the impacts of independent variables (cholesterol, Span 60, and soya lecithin) on the essential quality attributes—particle size, zeta potential, and drug release. Figure 27 (Cholesterol vs. Span 60) illustrates that the optimal region (yellow zone) is situated between cholesterol levels of 0.12–0.13 and Span 60 levels of 0.36–0.41, where all specified criteria are satisfied. The Cholesterol vs. Lecithin plot (Figure 27) indicates an optimal region at cholesterol levels of 0.13–0.14 and lecithin levels of 0.10–0.12. The most notable and sustained optimal region was identified in the Span 60 versus Lecithin plot (Figure 27), where the "sweet spot" closely matched the actual composition of Formulation Run 1, which demonstrated a high drug release (87%), favorable particle size (275 nm), and excellent zeta potential (-39 mV). The findings validate the robustness and predictive capability of the employed design model.

The optimal solution was demarcated in the design space overlay plot as shown in Figure 27(A,B&C)[44,45].

Percentage Entrapment Efficiency (% EE) of Optimised Formulation

The percent entrapment efficiency was found to be 70.79±5.63%. The reproducible results of entrapment efficiency is an indicator that the preparation method of Proniosomes is good and has the potential to be introduced for scalability. Moreover, entrapment efficiency also attributes towards the significant therapeutic performance of the drug loaded Nanoformulation.

In-vitro Release of Optimised Formulation and Comparative Study with Neat Formulation of Quercetin

Proniosomes formulation of quercetin displayed significant drug release due to solubility enhancement of the quercetin by Nano formulation. Specified controlled release of the drug was also observed from the Nano formulation with 53% and 84% drug release at 180 and 600 minutes respectively.

The study compared the drug release behavior of pure quercetin and a Proniosomes formulation (Figure 28). Pure quercetin had a restricted release, with a maximum cumulative release of 20% over 24 hours. Proniosomes formulation showed a rapid initial release followed by a sustained phase, resulting in nearly 100% cumulative release within 24 hours[46].

This improvement suggests Proniosomes improve the solubility and bioavailability of quercetin, making them a viable delivery system for topical or transdermal applications in psoriasis treatment. The results showed reproducibility, indicating the robustness and consistency of the developed formulation.

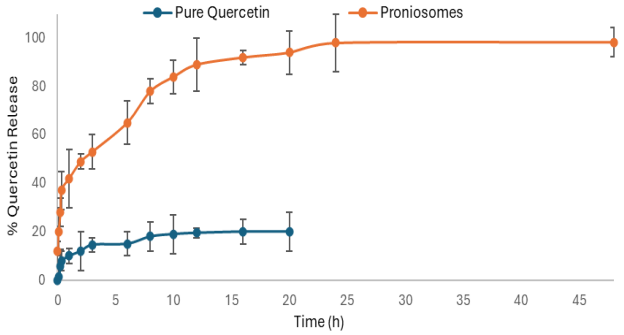

Figure 28: Comparative *in-vitro* release profile of quercetin from pure quercetin dispersion and quercetin-loaded Proniosomes over 48 hours

DISCUSSION

A delivery method that sustains localized medication concentrations at the skin lesion site is necessary for psoriasis, a skin disorder marked by persistent keratinocyte hyperproliferation and inflammatory signaling. By lowering oxidative stress and modulating NF-κB-driven inflammation, suspended release from proniosomes laden with quercetin stops keratinocyte rebound growth. For the long-term treatment of psoriasis, this extended-release/ sustained release profile is both pathophysiologically significant and pharmaceutically desirable.

Several nanocarrier systems, including liposomes, ethosomes, and nanoemulsions, have been previously investigated for dermal delivery of quercetin in psoriasis therapy. Liposomes improve drug entrapment and enhance penetration; however, their instability, high production costs, and short shelf life limit large-scale application. Ethosomes, enriched with ethanol, provide superior skin permeation compared to liposomes, but their high alcohol content often causes irritation, making them less suitable for chronic conditions such as psoriasis. Nanoemulsions offer enhanced solubility and permeation of hydrophobic drugs, but they are prone to phase separation and require stabilizers to maintain long-term integrity.

In contrast, Proniosomes combine the advantages of these systems while overcoming several limitations. They are dry, free-flowing powders that are hydrated into niosomes immediately before use, thereby offering superior stability, ease of storage, and scalability. Moreover, our optimized proniosomal formulation demonstrated sustained drug release, high entrapment efficiency, and favorable zeta potential—features that directly address the clinical need for prolonged quercetin delivery in hyperproliferative psoriatic skin. These attributes suggest that proniosomes may provide a more patient-friendly, stable, and clinically translatable nanocarrier compared to conventional vesicular systems.

CONCLUSION

The study developed and optimized quercetin-loaded Proniosomes as a promising vesicular drug delivery system for psoriasis management. The formulation showed high entrapment efficiency, enhanced stability, improved permeation, and sustained release compared to pure quercetin. The Proniosomes gel achieved 87% cumulative permeation over 24 hours, and it's *in-vitro* release profile improved significantly compared to pure quercetin. Further exploration is needed to establish their therapeutic efficacy and safety. Further exploration is warranted to further explore this promising herbal nanocarrier system.

However, while the *in-vitro* and *ex-vivo* findings are encouraging, further research is essential to translate these outcomes into clinical utility. Rigorous *in-vivo* studies are needed to validate the therapeutic efficacy of the formulation in relevant animal models of psoriasis. In

addition, systematic toxicity and safety assessments should be conducted to rule out any potential adverse effects associated with long-term use. Finally, well-designed clinical investigations will be crucial to determine pharmacokinetics, patient tolerability, and therapeutic outcomes in human subjects.

Overall, the present work lays a strong foundation for advancing quercetin-loaded Proniosomes from bench to bedside. With continued exploration through *in-vivo* validation, toxicity profiling, and clinical translation, this delivery system holds promise to emerge as a safe, effective, and scalable herbal nanotechnology-based intervention for psoriasis management.

Author Contributions

All authors have contributed in the composition of this article, all read entire content of this manuscript and approved final version for publication.

REFERENCES

1. Sugumaran D, Yong ACH, Stanslas J. Advances in psoriasis research: From pathogenesis to therapeutics. Life Sci. 2024 Oct;355:122991.
2. Michalek IM, Loring B, John SM. A systematic review of worldwide epidemiology of psoriasis. J Eur Acad Dermatology Venereol. 2017 Feb;31(2):205–12.
3. Luna PC, Chu CY, Fatani M, Borlenghi C, Adora A, Llamado LQ, et al. Psychosocial Burden of Psoriasis: A Systematic Literature Review of Depression Among Patients with Psoriasis. Dermatol Ther (Heidelb). 2023 Dec 23;13(12):3043–55.
4. Kamata M, Tada Y. Efficacy and Safety of Biologics for Psoriasis and Psoriatic Arthritis and Their Impact on Comorbidities: A Literature Review. Int J Mol Sci. 2020 Mar 1;21(5):1690.
5. Yamanaka K, Yamamoto O, Honda T. Pathophysiology of psoriasis: A review. J Dermatol. 2021 Jun 22;48(6):722–31.
6. Diotallevi F, Paolinelli M, Radi G, Offidani A. Latest combination therapies in psoriasis: Narrative review of the literature. Dermatol Ther. 2022 Oct 26;35(10).
7. Warzyszak P, Małek R, Milczek M, Żołyniak W, Tomasik M, Hawranik I, et al. Psoriasis - a review of recent progress, characteristics, diagnostic management. J Educ Heal Sport. 2022 Dec 27;13(2):149–55.
8. Thirumal D, Sindhu RK, Goyal S, Sehgal A, Kumar A, Babu MA, et al. Pathology and Treatment of Psoriasis Using Nanoformulations. Biomedicines. 2023 May 30;11(6):1589.
9. Sharma H, Gupta N, Garg N, Dhankhar S, Chauhan S, Beniwal S, et al. Herbal Medicinal Nanoformulations for Psoriasis Treatment: Current State of Knowledge and Future Directions. Nat Prod J. 2024 Oct;14(7).
10. Monga G, Kumar S, Dhamija I, Sindhu RK. Synergistic and enhanced therapeutic potential of a novel transethosomal curcumin-psoralen loaded formulation in psoriasis management. Biochem Cell Arch. 2024 Sep 25;24(2).
11. Shrivastav S, Sindhu RK, Kumar S, Kumar P. Anti-psoriatic and phytochemical evaluation of. Pharm Sci. 2009;1:176–85.
12. Su R, Zhao S, Zhang J, Cao M, Peng S. Metabolic influences on T cell in psoriasis: a literature review. Front Immunol. 2023 Nov 15;14.
13. Li T, Gao S, Han W, Gao Z, Wei Y, Wu G, et al. Potential effects and mechanisms of Chinese herbal medicine in the treatment of psoriasis. J Ethnopharmacol. 2022 Aug;294:115275.
14. Jo HG, Kim H, Lee D. Oral Administration of East Asian Herbal Medicine for Inflammatory Skin Lesions in Plaque Psoriasis: A Systematic Review, Meta-Analysis, and Exploration of Core Herbal Materials. Nutrients. 2022 Jun 12;14(12):2434.
15. Huang TH, Lin CF, Alalaiwe A, Yang SC, Fang JY. Apoptotic or Antiproliferative Activity of Natural Products against Keratinocytes for the Treatment of Psoriasis. Int J Mol Sci. 2019 May 24;20(10):2558.
16. Sindhu RK. Nanotechnology and drug delivery: Principles and Applications. Nanotechnol Drug Deliv Princ Appl. 2024 Jan 1;1–625.
17. Sultana S, Khan MR, Kumar M, Kumar S, Ali M. Nanoparticles-mediated drug delivery approaches for cancer targeting: A review. J Drug Target. 2013;21(2):107–25.
18. Jurel P, Bahadur S, Bajpai M. Herbal based nanoemulsions in psoriasis therapy: A review. Pharmacol Res - Nat Prod. 2024 Mar;2:100017.
19. Yadav T, Yadav HKS, Raizaday A, Alam MS. The treatment of psoriasis via herbal formulation and nano-polyherbal formulation: A new approach. BioImpacts. 2024 Aug 11;
20. Vora B, Khopade AJ, Jain N. Proniosome based transdermal delivery of levonorgestrel for effective contraception. J Control Release. 1998 Jul;54(2):149–65.
21. M. S, PANDA SP, BUDDHA S, KUMARI PVK, RAO YS. PRONIOSOMES: A VESICULAR DRUG DELIVERY SYSTEM. Int J Curr Pharm Res. 2021 Nov 15;32–6.
22. Ahmad MZ, Mohammed AA, Mokhtar Ibrahim M. Technology overview and drug delivery application of proniosome. Pharm Dev Technol. 2017 Apr 3;22(3):302–11.
23. Malgope A, Murthy PN, Ramani R, Dey S. Development of Nanoemulsion as Carrier for Transdermal Delivery of Valsartan. Int J Pharm Chem Sci. 2013;2(4):1655–65.
24. Jangam RP, Thombre AN, Gaikwad NP. A Review: Proniosomes as a Novel Drug Delivery System. Asian J Pharm Technol. 2017;7(3):166.
25. Madan JR, Ghuge NP, Dua K. Formulation and evaluation of proniosomes containing lornoxicam. Drug Deliv Transl Res. 2016 Oct 2;6(5):511–8.
26. Zhang Y, Gong S, Liu L, Shen H, Liu E, Pan L, et al. Cyclodextrin-Coordinated Liposome-in-Gel for Transcutaneous Quercetin Delivery for Psoriasis Treatment. ACS Appl Mater Interfaces. 2023 Aug 30;15(34):40228–40.
27. Topuzoğlu S, Yapar EA, Abdo L, Esentürk-Güzel İ, Yurtsever AG, Gümrükçü S, et al. Optimization and

Characterization of Khellin Loaded Nanogel for the Potential Use in Psoriasis Management. Curr Pharm Biotechnol [Internet]. 2025 May 6 [cited 2025 Jul 15];26. Available from: https://www.benthamdirect.com/content/journals/cpb/10.2174/0113892010375509250429052937
28. Ajrin M, Anjum F. Proniosome: A Promising Approach for Vesicular Drug Delivery. Turkish J Pharm Sci. 2022 Aug 31;19(4):462–75.
29. Rakesh K. Sindhu, Sumitra Singh EAY. John Wiley & Sons, 2025. 2025 [cited 2025 Jul 15]. Bioactive-Based Nanotherapeutics - Google Books. Available from: pJFGAdj6KpE_cE0F01M9pmsQ&redir_esc=y#v=onepage&q=Rakesh k Sindhu%2B psoriasis&f=false
30. Gupta A, Jain P, Nagori K, Adnan M, Ajazuddin. Treatment strategies for psoriasis using flavonoids from traditional Chinese medicine. Pharmacol Res - Mod Chinese Med. 2024 Sep;12:100463.
31. Hatahet T, Morille M, Hommoss A, Devoisselle JM, Müller RH, Bégu S. Liposomes, lipid nanocapsules and smartCrystals®: A comparative study for an effective quercetin delivery to the skin. Int J Pharm. 2018 May;542(1–2):176–85.
32. Ahmad A, Tiwari N. Development and Evaluation of Quercetin-Loaded Phytosomal Hydrogel for Psoriasis Therapy: A Review. Int J Pharm Res Appl. 2025 Jan;10(1):1296–8.
33. Botta L, Gatta G, Didonè F, Cortes AL, Pritchard-Jones K. International benchmarking of childhood cancer survival by stage at diagnosis: The BENCHISTA project protocol. PLoS One. 2022 Nov 1;17.
34. Putri VS. Validation of uv-vis spectrophotometric method to determine drug release of quercetin loaded-nanoemulsion. Indones J Pharm. 2022 Aug 15;
35. Srivastava N, Bansal A, Aggarwal K, Nagpal K. Development and Validation of UV Spectrophotometric Method for the Quantitative Estimation of Quercetin in Bulk Followed by Its Solubility Studies. J Appl Spectrosc. 2024 Jul 5;91(3):700–8.
36. Birla D, Khandale N, Bashir B, ShahbazAlam M, Vishwas S, Gupta G, et al. Application of quality by design in optimization of nanoformulations: Principle, perspectives and practices. Drug Deliv Transl Res. 2025 Mar 10;15(3):798–830.
37. Sayyad N, Maji R, Omolo CA, Ganai AM, Ibrahim UH, Pathan TK, et al. Development of niosomes for encapsulating captopril-quercetin prodrug to combat hypertension. Int J Pharm. 2021 Nov 20;609.
38. Thabet Y, Elsabahy M, Eissa NG. Methods for preparation of niosomes: A focus on thin-film hydration method. Methods. 2022 Mar 1;199:9–15.
39. Ravalika V, Sailaja AK. Formulation and Evaluation of Etoricoxib Niosomes by Thin Film Hydration Technique and Ether Injection Method. Nano Biomed Eng. 2017 Sep 30;9(3).
40. Kumar A, Goyal S, Kumar S, Singh S, Sindhu RK. Proniosome-based smart delivery systems for Psoriasis-targeted bioactive therapy. Journal of Integrated Science and Technology. 2025 Jun 9;13(7):1152.
41. Rashid M, AhmaD FJ, Alam S, Sindhu RK. Development and optimisation of nanoemulsion as carrier for cucurbitacin. Biochem Cell Arch [Internet]. 2023;23(S1):1465–73. Available from: https://connectjournals.com/pages/articledetails/toc037795
42. Luo Y. Chen J. Kuai L. Zhang Y. Ding X. Luo Y. Ru Y. Xing M. Li H. Sun X. Li B. Li X. Chinese herbal medicine for psoriasis: Evidence from 11 high-quality randomized controlled trials. *Front. Pharmacol.* 2021 11 599433 10.3389/fphar.2020.599433 3355180443.
43. Hindustan Abdul A, Golla Bala A, Chintaginjala H, Manchikanti SP, Kamsali A, Dasari RR. "Equator Assessment of Nanoparticles Using the Design- Expert Software." Int J Pharm Sci Nanotechnol. 2019 Oct 15;13(1):4766–4722.
44. Akram W, Garud N. Design expert as a statistical tool for optimization of 5-ASA-loaded biopolymer-based nanoparticles using Box Behnken factorial design. Futur J Pharm Sci. 2021 Dec 21;7(1):146.
45. Bayat F, Dadashzadeh S, Aboofazeli R, Torshabi M, Baghi AH, Tamiji Z, et al. Oral delivery of posaconazole-loaded phospholipid-based nanoformulation: Preparation and optimization using design of experiments, machine learning, and TOPSIS. Int J Pharm [Internet]. 2024 Mar 25 [cited 2025 Jul 15];653:123879.
46. Kumar N, Gupta G, Singh A, Sindhu RK, Rashid M. 4-Hydroxyisoleucine-Loaded Nanogel : Development from an Optimized Nanoemulsion for Antidiabetic Therapy. Int J Drug Deliv Technol. 2025;15(2):641–89.